EFFECT OF RUPTURE IN A FISSION GAS HOLDUP BED*

Dwight W. Underhill
Harvard School of Public Health
665 Huntington Avenue
Boston, Massachusetts 02115

Abstract

A gas adsorption bed operated under pressure will lose a por-
tion of the adsorbed gases in the event of an accidental rupture
of the container and release of pressure. Theoretical and labora-
tory studies show that the fractional release of fission gases will
be smaller than the ratio of the initial to the final bed pressure
and that the fraction of krypton released will be greater than the
fraction of xenon released under the same conditions.

I. Introduction

Currently the short lived isotopes of krypton and xenon con-
stitute the bulk of the radioactivity released to the atmosphere
from nuclear reactors. The release of gases contaminated with
these radionuclides may be delayed by a holdup system, and if the
holdup time is sufficiently long (e.g., 120 days), the off gas
stream may be effectively decontaminated of all short lived fis-
sion gas nuclides. The ten year nuclide, ^{85}Kr, cannot be controlled
by such a holdup system, but fortunately the fission yield of this
nuclide is small. A major problem in the design of a fission gas
holdup system is the space required for an effective system. The
required storage volume may be reduced considerably either by
filling the holdup tanks with an adsorbent material (such as char-
coal) and/or by operating the system under pressure. Operation
under pressure, however, presents the potential situation in which
the bed develops an accidental leak with total loss of pressure
and accompanying release of a portion of the adsorbed gases. This
paper presents an evaluation of this type of accident taking place
in a pressurized bed filled with adsorbent. The study was per-
formed by the author in conjunction with the design of a fission
gas holdup system for the Fast Flux Test Facility.

II. Accident Considerations

Several types of releases are possible in the case of the
development of a leak in a pressurized bed. But a violent rupture

in which the bed container essentially disintegrates with portions
of the adsorbent ejected appears highly unlikely because the max-
imum operational pressure generally considered for such a bed would
be restricted to eleven atmospheres (absolute) or lower. A more
probably accident situation is a slow leak, and in this case, the
most important points to consider are:

a.   In the presence of an adsorbent, the fission gases, kryp-
ton and xenon, are much less mobile than their carrier gas (which
for the FFTF off gases will be argon). For this reason, it would
appear that the fraction of fission gases escaping from the bed
will be significantly smaller than the fraction of carrier gas.

b.   As a result of radiodecay at steady state, the concentra-
tion of fission gas will be highest near the bed inlet and lowest
near the bed outlet. If a leak develops near the feed input, the
possibility exists that only a small release of carrier gas could
sweep out an appreciable fraction of the fission gases contained
within the bed.

The net effect of these two opposing factors on fission gas
leakage can be calculated on the basis of the analysis developed
below.

III.   Development of Theory

To establish a model for numerical analysis, we assume that
there is a rupture at or near the entrance to the bed diagrammed
in Figure 1. As was pointed out above, this would be the point
of highest fission gas concentration within the bed and would,
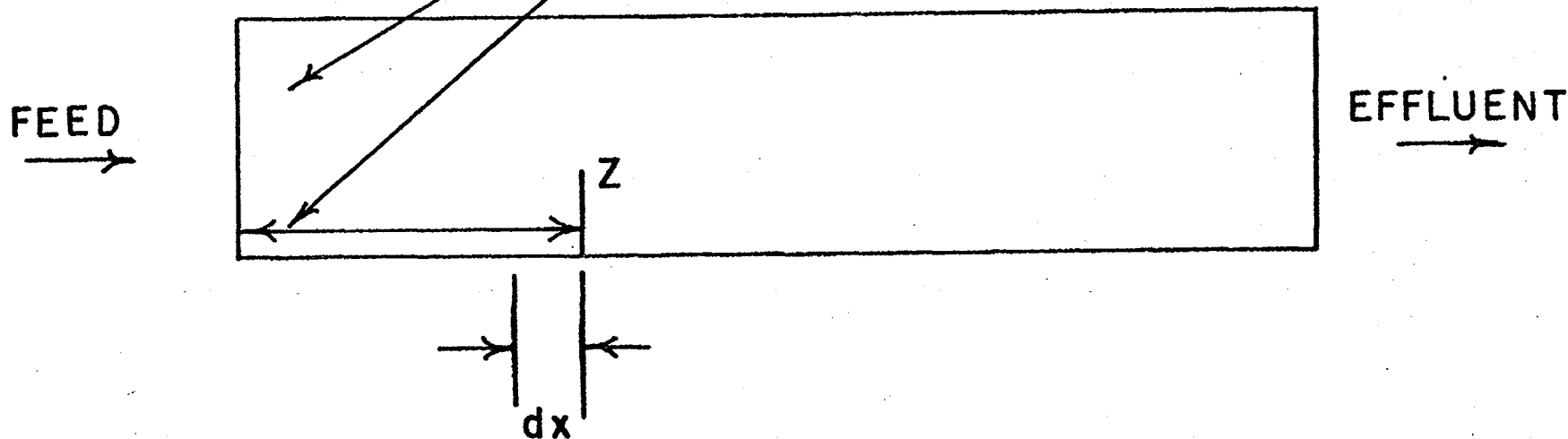therefore, be the point where maximum release would occur.

The fission gas adsorbed in the bed nearest the point of rup-
ture will be swept out of the bed by the escaping gases, whereas
the fission gas adsorbed deepest in the bed will be retained. The
first example considered here is a bed in which a leak develops at
the bed inlet (the point x=0 in Figure 1). The analytical pro-
cedure used here is to find the point, z, in the bed dividing the
fission gas which escapes from that which is retained. The follow-
ing assumptions have been made in locating the point,z.

a.   the release occurs under isothermal conditions;

b.   the fission gases are highly diluted by the carrier gas;

c.   both the fission gas and the carrier gas follow linear
     adsorption isotherms; and

d.   the pressure release is confined to a single bed.

Under these conditions, the instantaneous flow of all gases
at any point in the bed is proportional to the distance from the
point, L, which represents the effluent end of the bed. Also, the
instantaneous flow velocity of a fission gas is equal to the
instantaneous flow velocity of the carrier gas divided by the ratio

FIGURE I

REGION OF HIGHEST FISSION
GAS CONCENTRATION

FEED

EFFLUENT

Z

dx

DIAGRAM OF FISSION GAS ADSORPTION BED

of their adsorption coefficients. It follows directly that the differential equation giving the distance moved by the carrier gas is:

$$- \frac{d(L-x)}{L-x} = \frac{dP}{P},$$ (1)

where P = absolute pressure in the bed, and further the incremental distance moved by a fission gas is given by:

$$- \frac{d(L-x)}{L-x} = \frac{dP}{aP}$$ (2)

where a = ratio $\left\{\dfrac{\text{adsorption coefficient for fission gas charcoal}}{\text{adsorption coefficient for carrier gas charcoal}}\right\}$.

On integration, Equation (2) becomes

$$\int_z^0 - \frac{d(L-x)}{L-x} = \int_{P_i}^{P_{atm}} \frac{dP}{aP}$$ (3)

where P_{atm} = atmospheric pressure

P_i = initial pressure.

Then

$$\ln\left(\frac{L-z}{L}\right) = \frac{1}{a} \ln\left(P_{atm}/P_i\right)$$ (4)

or

$$z = L\left\{1 - \left(\frac{P_{atm}}{P_i}\right)^{1/a}\right\}$$ (5)

During normal operation, the radioactive fission gases will have an exponential decrease in activity as a result of natural decay while passing through the bed. Therefore, it can be assumed that the distribution of fission gas activity as a function of distance from the entrance can be expressed as: $g(x) = be^{-\alpha x}$.

Whatever the function $g(x)$ is, the fraction, f, of a fission gas nuclide released from the bed will be

63

$$f = \left. \int_0^z g(x)dx \middle/ \int_0^L g(x)dx \right. \tag{6}$$

When $g(x) = be^{-\alpha x}$,

$$f = \frac{1-e^{-\alpha z}}{1-e^{-\alpha L}} \tag{7}$$

or substituting the value for z,

$$f = \frac{1-e^{-\alpha L\left\{1-\left(\frac{P_{atm}}{P_i}\right)^{1/a}\right\}}}{1-e^{-\alpha L}} \tag{8}$$

When $\alpha L \ll 1$, only a small fraction of fission gas undergoes decay while passing through the bed and a nearly even initial distribution of fission gas across the bed results. For this condition, the equation for f reduces to

$$f = 1 - \left\{\frac{P_{atm}}{P_i}^{1/a}\right\} \tag{9}$$

which is essentially the equation derived by Jury[1] for a release from an adsorption bed having a uniform initial distribution of dilute fission gas.

For the case of ideal mass transfer[2]

$$\alpha = \frac{\lambda \rho K_o (\text{fission gas})}{V_s} \tag{10}$$

and

$$a = \frac{K_o(\text{fission gas})}{K_o(\text{carrier gas})} \tag{11}$$

where

ρ = density of the adsorbent, gms/cm^3

K_o = adsorption coefficient, cm^3/gm

V_s = superficial carrier gas velocity, cm/sec

λ = isotopic decay constant, sec^{-1}

The bulk adsorption coefficient, K_o, can be defined in many ways: to avoid confusion, K_o is defined here as the volume of a gas in a gram of bulk adsorbent measured at the partial pressure of the gas in the adsorbent. With this definition and the previous assumption of a linear isotherm, the bulk adsorption coefficient, K_o, becomes independent of the partial pressure of the adsorbed gas. The superficial velocity, V_s, is assumed to be measured at the pressure inside the bed before the rupture occurred.

IV. Experimental Results

The theory presented here was tested on a laboratory scale by measuring the fractions of ^{85}Kr and ^{133}Xe released from a charcoal bed following a sudden loss of pressure. The experimental procedure was to pass, under pressure at room temperature, argon plus trace quantities of either ^{85}Kr or ^{133}Xe, through a charcoal bed until the effluent concentration equaled the input concentration. At this point the bed was saturated with the fission gas, and the bed was then isolated and depressurized. The adsorption coefficient for argon could be determined from the volume of argon released from the bed. The activity of the fission gas in the released argon was also measured. By sweeping the bed with uncontaminated argon, the residual activity of the fission gas in the bed was also found, and from the total amount of fission gas in the bed, at saturation, the adsorption coefficient for the fission gas was also calculated. Thus, during a single run, both fractional release of fission gas, as well as all the parameters needed to calculate the theoretical fission gas release, were measured. Table 1 gives the experimental and theoretical fission gas releases for ^{85}Kr and ^{133}Xe from beds pressurized to 2 and to 10 atmospheres (gage).

As predicted from theory, the fractional release of fission gases was smaller than the ratio of the initial to the final bed pressure. Also, as predicted, the fraction released increased with initial pressure, and under similar conditions, the fraction of krypton released was significantly greater than the fraction of xenon released.

It is important to note that the observed releases were somewhat less than those calculated from the assumption of an isothermal release. The fact is that the desorption of large volumes of the argon carrier gas resulted in a simultaneous cooling of the beds during the depressurization, and this cooling in effect changed the value of the parameter "a" during the release. The analysis could

TABLE 1

FRACTIONAL RELEASE OF FISSION GASES FOLLOWING RAPID DEPRESSURIZATION

Carrier Gas: Argon; Temperature: Ambient

Run	Fission Gas	Weight of Charcoal in Bed	Initial Pressure (gage)	Observed Fractional Release	Predicted Fractional Release
1	^{85}Kr	480g	30 psi	0.16	0.21
2	^{85}Kr	480g	30 psi	0.14	0.18
3	^{85}Kr	480g	150 psi	0.32	0.48
4	^{85}Kr	480g	150 psi	0.34	0.46
5	^{133}Xe	480g	30 psi	0.011	0.016
6	^{133}Xe	480g	30 psi	0.008	0.011
7	^{133}Xe	144g	150 psi	0.018	0.048
8	^{133}Xe	144g	150 psi	0.017	0.046

be altered to take this effect into account, but such a procedure would then not be valid for a slow, isothermal release. For this reason we propose that the simple formulas developed here be retained with the understanding that for sudden releases they may be somewhat conservative.

V. Sample Calculations

To demonstrate typical fission gas release values based upon the theory developed above, sample calculations were performed for the situation assumed to exist in a bed pressurized to 10 atmospheres (gage).

In a set of sample data for operation of a holdup bed at ambient temperature (25°C)

$$\rho = 0.48 \text{ gm/cm}^3$$

$$K_o = 357 \text{ cm}^3\text{/gm for Xe}$$

$$= 28 \text{ cm}^3\text{/gm for Kr}$$

$$= 6.64 \text{ cm}^3\text{/gm for Ar}$$

$$V_s = 0.25 \text{ cm/sec}$$

$$L = 300 \text{ cm}$$

$$P = 10 \text{ atmospheres (gage)}$$

Table 2 gives the curies/sec, $\dot{q}$, for each radionuclide in the feed to the bed. This rate of release is calculated from an FFTF Deisgn assuming four 2 MW closed loops and 1% defected fuel in reactor. From Equation (12) the activity of each nuclide in the holdup bed can be calculated.

$$q = \frac{\dot{q}}{\lambda} (1-e^{-\alpha L}) \tag{12}$$

where q equals the curies of each nuclide contained in the bed. From Equation (8) the fractional release of each nuclide is calculated, and this as well as the total release is also given in Table 2. By an analogous procedure the fission gas release from a leak in the middle or at the outlet of the bed was calculated and the results are also given in Table 2.

VI. Commentary and Conclusions

As may be noted from Table 2, the development of a leak in a fission gas holdup bed, pressurized to 10 atm (gage) and operating under equilibrium conditions, will results in a greater fractional release of the krypton isotopes. This is as would be expected because of the greater mobility of this gas. Further, if the leak occurs near the bed input, there is a greater fractional release

TABLE 2

CALCULATED RELEASES FROM A FISSION GAS HOLDUP BED

Initial Pressure: 10 atm (gage)

Nuclide	Input Curies/Day	Curies in Bed at Steady State	Site of Rupture					
			Input End		Middle of Bed		Effluent End	
			Fraction Released	Curies Released	Fraction Released	Curies Released	Fraction Released	Curies Released
^{131m}Xe	139.2	309.5	0.046	14.41	0.043	13.49	0.040	12.63
^{133m}Xe	3369.0	5726.8	0.060	344.35	0.042	244.56	0.030	173.69
^{133}Xe	67650.0	138408.4	0.050	6975.68	0.043	6013.14	0.037	5183.61
^{135}Xe	342000.0	186818.3	0.173	32375.20	0.022	4146.54	0.002	531.08
^{83m}Kr	23586.0	2140.7	0.634	1358.79	0.395	847.01	0.246	527.99
^{85m}Kr	39150.0	5244.5	0.520	2730.91	0.426	2236.86	0.349	1832.20
^{85}Kr	2.6	0.5	0.432	0.21	0.423	0.20	0.428	0.21
^{87}Kr	67920.0	5027.9	0.697	3506.15	0.367	1850.02	0.194	976.16
^{88}Kr	82440.0	9302.5	0.569	5299.35	0.416	3872.34	0.304	2829.60

of shorter lived radionuclides. Since these nuclides constitute the bulk of the radioactivity near the area of the assumed leak, this situation is as would be expected.

The overall release of fission gases is calculated to be 14.9 per cent of the total radioactivity contained within the bed if the release occurs near the bed input. Similar calculations for assumed leaks in the middle and near the outlet end of the bed showed radionuclide releases only of 5.4 and 3.4 percent, respectively of the total radioactivity contained within the bed.

Furthermore, if the adsorption bed were to be operated at cryogenic temperatures, the ratio of adsorption coefficients (the factor "a") would increase substantially. Under these conditions, the fraction of fission gases released from a bed could be significantly smaller than those calculated here. In addition, we have assumed an initial pressure of 10 atmospheres (gage). For operation at lower pressures, smaller fractional releases on depressurization would be expected.

References

1. Jury, S. H., "Design of Percolators", USAEC Report CF-51-7-41, (1951).

2. Underhill, D. W., "A Mechanistic Analysis of Fission Gas Holdup Beds, Nuclear Applications, Vol. 6, p. 544, (June, 1969).

DISCUSSION

JONAS: In order to integrate the right side of your equation you would have to assume that "a" was not a function of the pressure changes?

UNDERHILL: This would be the case for linear isotherms.

JONAS: It would also indicate that the isotherms of the fission gas and the carrier gas were approximately the same. I wonder if that was one of the causes for the variance between the observed and calculated data.

UNDERHILL: We know from the results of Förster and some other work we did, that there is a change in the adsorption coefficient of krypton at high pressures. I think there is probably some effect of this in the results. But, again, there was a very, very strong cooling effect and I think that was the primary reason for the deviation between theory and experiment.

JONAS: Yes; I agree. I guess what I was pushing for is the question of whether the cooling effect is adding to or subtracting from the deviations.

UNDERHILL: I see your question, and it's really an unanswerable one, unless we do further research.

WYMER: You talk about rapid depressurization. I wonder how rapid; and how did you do it experimentally?

UNDERHILL: We simply opened up a valve, releasing everything through a quarter-inch copper tubing.

WYMER: How long did it take?

UNDERHILL: There was an initial swoosh of material and then we waited about two hours to allow the temperature of the bed to become the ambient temperature.

WYMER: You mean a one-second swoosh or a two-second swoosh?

UNDERHILL: It's hard to say.

MICHELS: Have you considered the case in which the bed ruptures and you have a gas stream flowing over the charcoal?

UNDERHILL: Probably we could have, but we haven't considered that case up to now.

MASS AND HEAT TRANSFER OF KRYPTON-XENON ADSORPTION ON ACTIVATED CARBON

J. L. Kovach
E. L. Etheridge

Nuclear Consulting Services Inc.
P. O. Box 29151
Columbus, Ohio 43229

Abstract

A large number of boiling water reactors are being equipped with ambient temperature-carbon adsorption off-gas systems. The selection of adsorbent for these systems is often based on limited experimental data resulting in non-optimized processes. The data presented here was generated to assist in the selection of the adsorbent and operating conditions for the off-gas systems utilizing the ambient or near ambient adsorption process.

I. Carbon Optimization.

The adsorption of krypton and xenon on various
adsorbents has been extensively studied in the
past. Most investigators have used only one
adsorbent, or adsorbents of very widely varying
properties; therefore, the resulting data did not
permit optimization of a single base adsorbent. (1)

Although Lad and Young reported that lower surface
area identical base adsorbents exhibited higher
capacity toward xenon at low concentrations than
high surface area carbons and Mahajan and Walker
reported similar results for krypton adsorption
on activated carbons, many investigators selected,
and most results were reported on, high surface
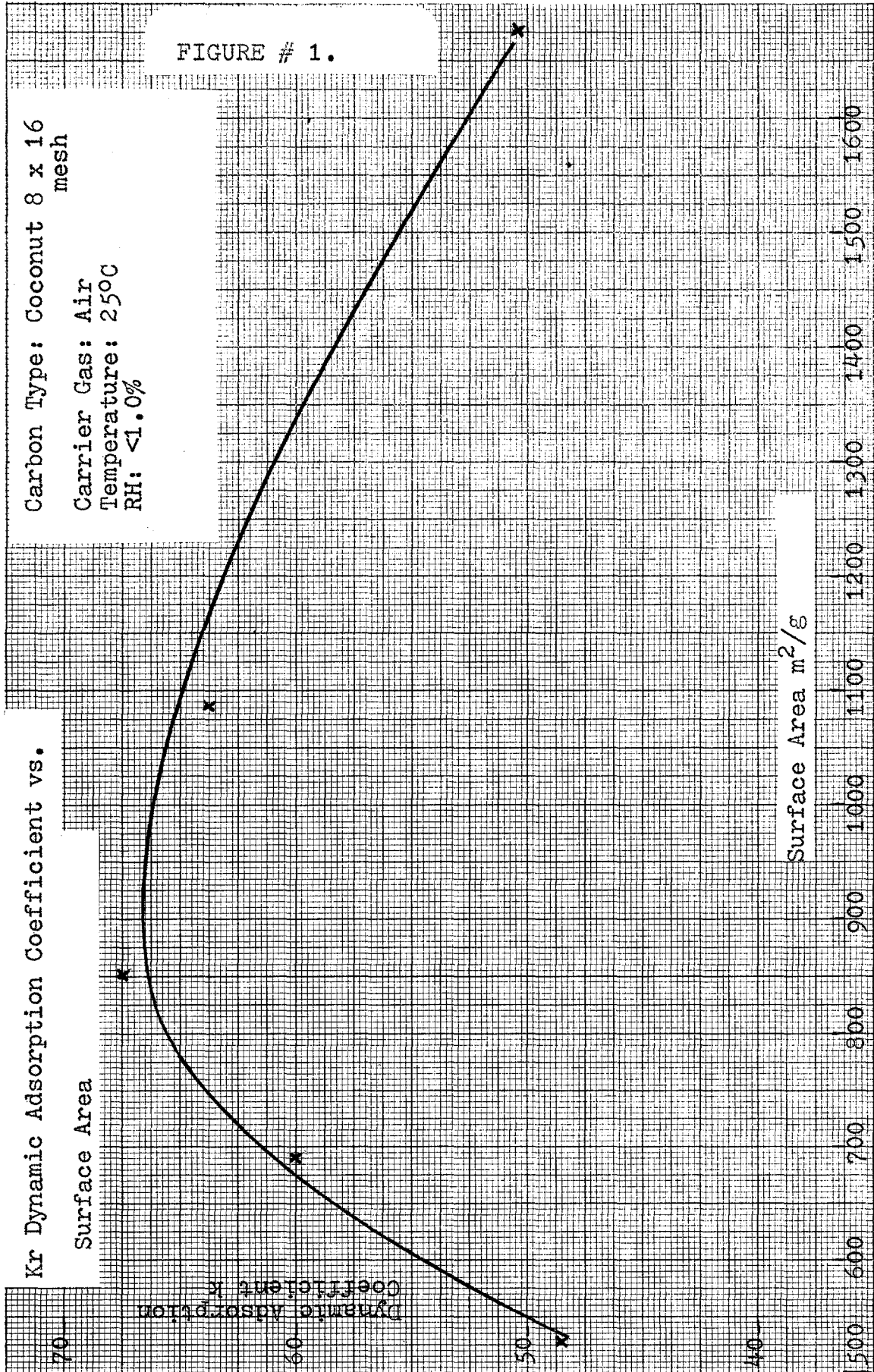area adsorbents. (2) (3)

The experiments to evaluate optimum surface area
were performed on steam activated coconut base
carbons, subjected to various activation levels.
The carbons used had surface areas of 525 ± 50 m^2/g,
680 ± 50 m^2/g,
850 ± 50 m^2/g,
1085 ± 50 m^2/g,
1670 ± 75 m^2/g

using the BET nitrogen adsorption method.

The dynamic adsorption coefficients were determined
using Kr-85 tracer at 0.001 mmHg pressure in air.
The column dimensions were 6.0 inch ID and 3 foot
bed depth. The temperature was 25°C, the superficial
velocity 2 fpm and the relative humidity was kept
below 1.0%. The carbon adsorbents used were equi-
librated with tracer free air under the experimental
conditions. An Overhoff & Associates Model 120 ion
chamber was used to monitor Kr-85 breakthrough.

The obtained experimental data is shown on Figure
No. 1. The optimum surface area of this adsorbent
series is near 800 m^2/g for krypton adsorption
delay. The probable reason for the observed phenom-
enon is that during the activation process not only
the surface area increases but the pore size distri-
bution of the activated carbon also increases.
During the first phase of the activation process
new pores are developed while in successive stages
of the activation the pore size is enlarged. Due
to the fact that particularly at low concentration
adsorption takes place preferentially in the smallest
diameter pores, the use of the lower surface area
adsorbent is advantageous if the pore diameters

FIGURE # 1.

Carbon Type: Coconut 8 x 16 mesh

Carrier Gas: Air
Temperature: 25°C
RH: <1.0%

Kr Dynamic Adsorption Coefficient vs. Surface Area

Surface Area m²/g

Dynamic Adsorption Coefficient k

are small. Mahajan (3) evaluated carbonaceous
molecular sieves also showing that if by unique
processing the pore diameter can be kept small,
even at higher surface areas, a superior carbon
can be developed for krypton adsorption. However,
the preparation of carbonaceous molecular sieves
at the present time is not an economically compet-
itive process. Thus based on the experimental
results, the optimum pore diameter for krypton
adsorption, in steam activated coconut carbons,
is developed at approximately 800 m^2/g and further
increase in surface area does not result in increased
delay times due to the enlargement of the pores.
Literature data (4) does indicate that under cry-
ogenic conditions this relationship between pore
diameter and krypton, xenon delay times is not
valid. The temperature dependence of this rela-
tionship is being evaluated at the present time.

Even more significant differences are observed if
the Kr or Xe dynamic k is based on adsorbent volume
rather than weight. The surface area of activated
carbons is inversely proportional to their apparent
density; therefore the volumetric Kr-Xe adsorption
capacity shows even more advantage for using the
higher density, lower surface area coconut carbons.

The position of the krypton and xenon adsorption
isotherms determined under static conditions also
changes relative to each other on various pore
diameter and surface area carbons. Therefore it
is important that any single concentration point
evaluation is performed at or as close to the actual
concentrations as possible. To demonstrate this
concentration dependence, literature data plot
obtained under various concentrations on the iden-
tical adsorbent is shown on Figure No. 2. The
data was obtained under dynamic conditions from
argon carrier gas. (5)

The data indicates that contrary to other data the
slope of the adsorption isotherm, i.e. both the
static and dynamic k, changes even at the very
low noble gas concentrations.

II. Dynamic Considerations.

As was shown in an earlier report (6), the movement
of a noble gas molecule through the adsorbent bed is
also dependent on the slope of the adsorption iso-
therm, i.e. the dynamic (or static) adsorption
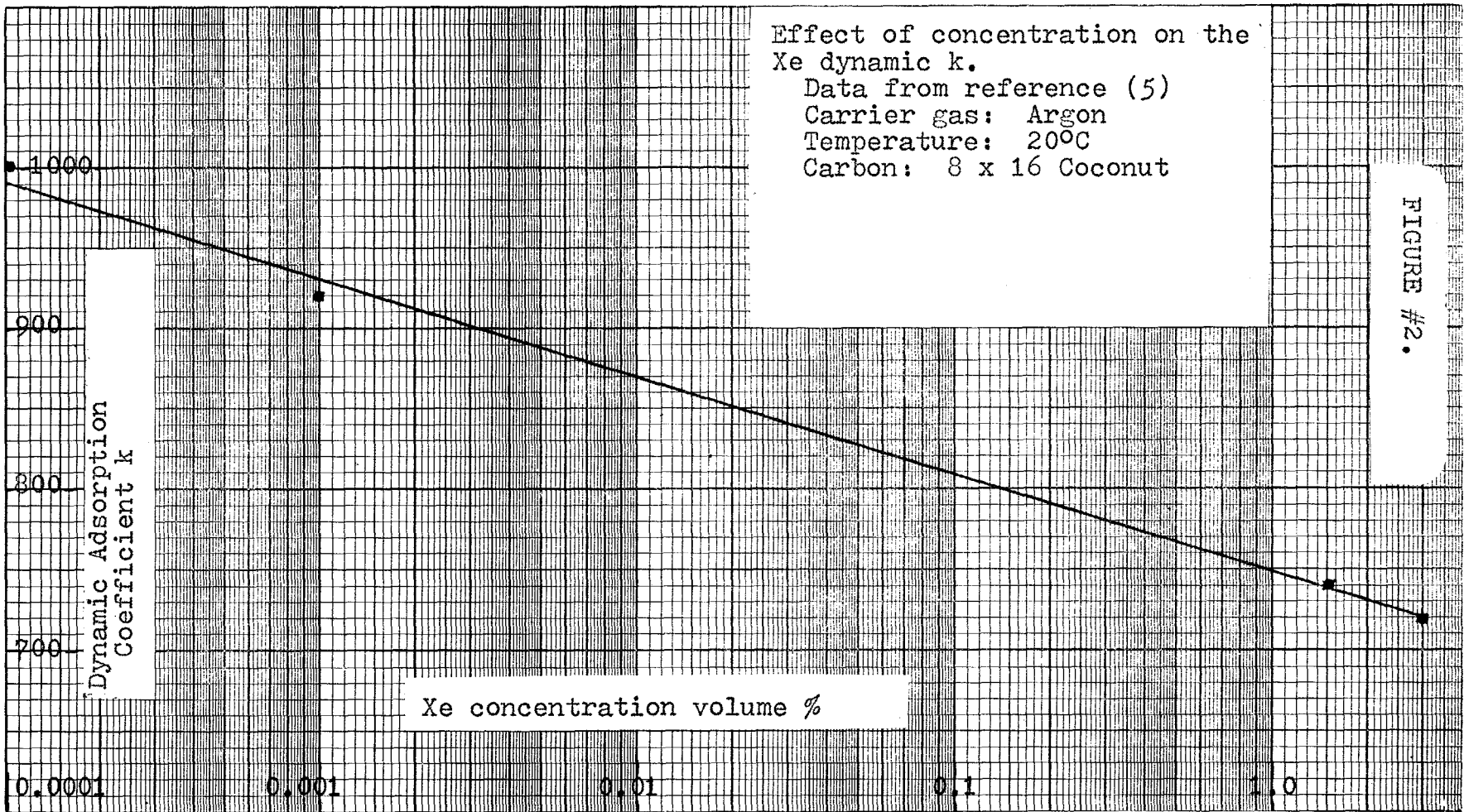coefficient k.

Effect of concentration on the Xe dynamic k.
Data from reference (5)
Carrier gas: Argon
Temperature: 20°C
Carbon: 8 x 16 Coconut

FIGURE #2.

12th AEC AIR CLEANING CONFERENCE

77

The rate of movement of the adsorption mass transfer zone in case of fixed superficial velocities is a function of the distribution of the adsorbate (in this case Kr and Xe) between the carbon and the gas phase.

$$u = v \, \frac{1}{a/P_o \, \epsilon} \, . \qquad\qquad [1]$$

The proportionality factor $a/P_o\epsilon$, giving the distribution of the Kr and Xe between the adsorbed and the gas phase, can be substituted by the adsorption coefficient k if the adsorbate quantity in the void volume is negligible, resulting in

$$u \approx q \, \frac{1}{k} \, . \qquad\qquad [2]$$

Thus the rate of movement of the adsorption mass transfer zone, i.e. the rate of movement of the Kr or Xe molecules through the adsorbent bed, will be accelerated by increasing the superficial velocity and will be decreasing in proportion to the adsorption coefficient.

If the adsorption isotherms of the particular adsorbate-adsorbent system are nonlinear over wide ranges, the nearest available data range k value can only be substituted.

At low gas velocities, particularly when using ion chambers which may dilute adsorbate concentrations, twin columns of two different bed lengths should be used. The obtained results

$$u = \frac{L_2 - L_1}{t_2 - t_1} \approx q \frac{1}{1 + k} \qquad [3]$$

will give more precise approximation of the rate of mass transfer zone movement.

Under very low velocity conditions, resulting in u of less than 3 cm/min Kr and Xe mass transfer zone movement in activated carbon beds, the longitudonal diffusion in the adsorber considerably increases the length of the mass transfer zone. Similar results were reported by Illes for CO_2, C_2H_2, C_2H_6 and C_3H_8 adsorption on activated carbon. (7)

III. Heat Transfer in Carbon Beds.

Although numerous correlations exist for packed granular bed heat transfer data, the mass velocity in these correlations was obtained at high Reynolds numbers. A theoretical derivation was developed to show the heat transfer coefficient versus gas velocity dependency through a wide velocity range. (8)

The equation representing the derivation

$$Nu = 0.2 + 0.03Pr^{0.33}Re^{0.54} + 0.35Pr^{0.356}Re^{0.58} \quad [4]$$

was evaluated in a 6.0 inch ID 3 foot long jacketed vessel. Figure No. 3 shows the curve corresponding to equation [4] and the data points obtained experimentally on an 8 x 16 mesh carbon in the 40°-100°C range in nitrogen. The following parameters were used or measured.
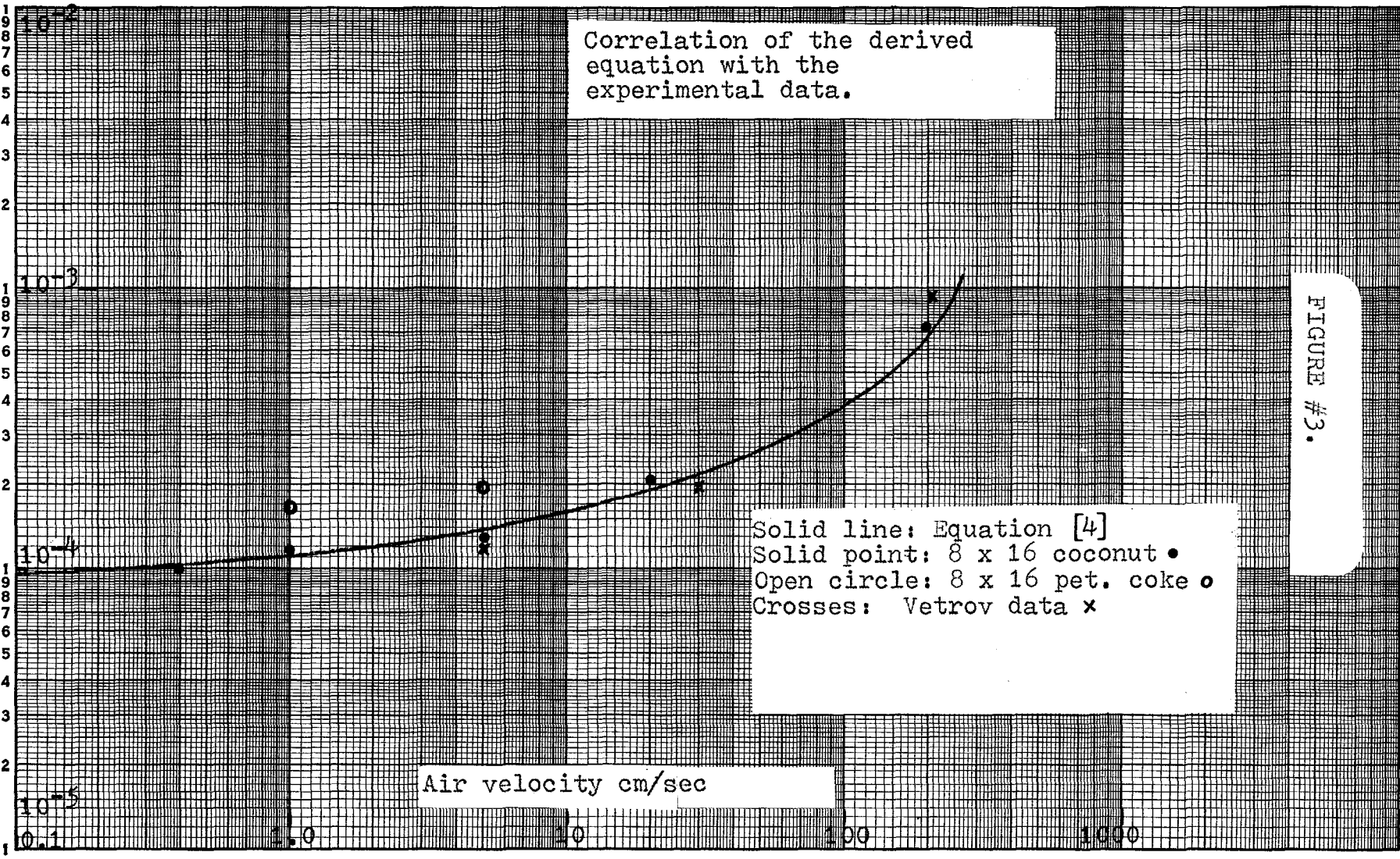
Average particle size:	0.128 cm
Average particle surface:	0.10 cm^2
Average particle volume:	0.002050 cm^3
Average number of particles:	278
Bed void fraction:	0.42
Surface area external:	27.0 cm^{-1}
Sphericity:	0.719
Carbon thermal conductivity:	3.10 x 10^{-4} cal/(cm)(sec)(°C) at 100°C
Carbon heat capacity:	0.20 cal/(g)(°C) at 100°C
Prandtl No.:	0.659
Reynolds No.:	0.777v

Correlation of the derived
equation with the
experimental data.

Solid line: Equation [4]
Solid point: 8 x 16 coconut •
Open circle: 8 x 16 pet. coke o
Crosses: Vetrov data x

Air velocity cm/sec

FIGURE #3.

The values reported by Vetrov (9) for chips and
steel shot were also plotted and show close agree-
ment with the obtained data. The developed equation
[4] agrees in order of magnitude with the conven-
tional (Wilke-Hougen, Gamson-Hougen, Colburn-Chilton,
etc.) equations only in the turbulent flow and very
low velocity ranges. The values observed exclude
any oxidation effects which may occur at high temper-
atures (above 120°C) in oxygen or oxidizing agent
containing carbon beds.

Equation [4] confirmed by experimental data, results
in a shape which points out the nonlinearity of the
heat ransfer coefficient-air velocity relationship
over the turbulent, intermediate, laminar flow and
"chimney effect" velocity ranges.

A limited number of experiments were performed using
near spherical carbon particles of similar size and
properties as the average size of the coconut shell
carbon used. The data resulted in slightly higher
α values than those obtained with the prismatic
shape coconut carbon even when the latter is sub-
jected to sphericity correction.

Whether this phenomenon is caused by the variation of the angle of attack or by the packing density difference in the non-uniform size coconut carbon beds is not clear at this time.

Summary.

The influence of carbon adsorbent structural properties were evaluated for noble gas removal systems. The effect of the obtained adsorption coefficients is discussed in relation to the movement of the mass transfer zone through the adsorbent bed. A heat transfer equation is presented for heat transfer on packed carbon beds; the equation is substantiated by measured data points and literature values.

Symbols.

a = volume of adsorbate adsorbed in 1 cm^3 adsorbent cm^3/cm^3.

k = adsorption coefficient, volumetric cm^3/cm^3.

L = adsorbent bed length cm.

P_0 = adsorbate concentration fraction at inlet cm^3/cm^3.

q = true velocity through the adsorbent bed cm/min.

t = time elapsed to breakthrough minutes.

u = rate of movement of the adsorption wave front cm/min.

v = superficial velocity of the carrier gas cm/min.

α = film heat transfer coefficient $cal/(cm)^2(sec)(^oC)$.

ϵ = void fraction of adsorbent bed cm^3/cm^3.

References.

(1) Kovach, J. L. Krypton and Xenon Adsorption
     Bibliography, Part I.
     NUCON Report 003 (June 1972).

(2) Lad, R. A. & Young, T. F. Adsorption of Xenon
     on Charcoals at Room Temperature.
     USAEC Report NNES IV-9 (Book 3, Part VII)
     (1951).

(3) Mahajan, O. P. & Walker, P. L., Jr. Krypton
     Adsorption on Microporous Carbons and 5A
     Zealite. Jour. Coll. Interface Sci. (29)
     129-137 (1969).

(4) Ackley, R. D. & Browning, W. E. Equilibrium
     Adsorption of Krypton and Xenon on Acti-
     vated Carbon and Linde Molecular Sieves.
     USAEC Report ORNL CF 61-2-32 (Feb. 1961).

(5) Collins, D. A. et al. The Adsorption of Krypton
     and Xenon from Argon by Activated Carbon.
     UKAEA Report TRG 1578 W (Sept. 1967).

(6) Kovach, J. L. Review of Krypton-Xenon Adsorber
     Design. NACAR Report 010005 (June 1970).

(7) Illes, V. Investigation of the Laws of Dynamic
     Adsorption. Doctoral Dissertation (1961).

(8) Kovach, J. L. Heat Transfer in Activated Carbon
     Beds. NUCON Report 017 (Aug. 1972).

(9) Vetrov, B. N. & Todes, O. M. Thermal Wave
     Propagation in Packed Beds in Flowing Gas.
     Zhur. Tech. Phys. (25) 1242 (1955).

DECONTAMINATION OF HTGR REPROCESSING OFF-GASES[*]

M. E. Whatley, R. W. Glass, P. A. Haas, A. B. Meservey, and K. J. Notz

Oak Ridge National Laboratory
Oak Ridge, Tennessee

Abstract

The off-gas from the reprocessing of HTGR fuel is unique among nuclear fuel reprocessing off-gases because of the large amount of CO_2 produced by the burning of the fuel element. An HTGR fuel element contains about ten times as much graphite as heavy metals. The relatively high temperature of the burning process ($\sim$800°C) releases virtually all of the volatile fission products, as well as troublesome amounts of some which are normally solid. There are filters for removing particulate solids and sorption methods for removing I_2 and ^3H_2O which have good potential for application to this off-gas, but no existing technology was found to remove and concentrate the Kr. The high concentration of CO_2 in the filtered gas stream ($\sim$90% CO_2, 10% light gases, 10-20 ppm Kr) and the similarity of CO_2 behavior to that of Kr preclude the use of commonly employed processes such as membrane permeation, sorption on charcoal or molecular sieves, and physical absorption by a third component. The removal of CO_2 before such an operation appears feasible, but undesirable. A process involving Kr Absorption in Liquid CO_2 (KALC), which exploits the fact that Kr is more soluble in liquid CO_2 than is O_2, N_2, or CO, appears to be a natural solution to this particular problem.

The solubility of Kr in liquid CO_2 was experimentally determined by an in situ radioactive counting method using ^{85}Kr. This method avoided the problems usually associated with sampling systems of highly volatile components. Krypton tracer and CO_2 were contained in a sealed stainless steel tube, brought to equilibrium by rocking in a constant-temperature bath, and counted with the tube in a vertical position to measure the radioactivity in each phase. Data were obtained at various temperatures over the entire CO_2 liquid range.

Engineering calculations, based on literature values for the solubilities of O_2, N_2, and CO and the measured values for Kr, were made for a KALC system which employs a fractionator, a stripper, and an absorber. These calculations indicate that 99.9% of the Kr in the off-gas stream can be concentrated into a very small volume.

The Rare Gas Removal Pilot Plant at the ORGDP was used to explore the feasibility of operating a KALC system. In addition to demonstrating feasibility, the initial pilot campaign provided encouragement that the KALC process is a good way to decontaminate the HTGR reprocessing off-gases.

Introduction

The off-gas from the reprocessing of HTGR fuel elements is unique among processing plant off-gases because the graphite and other carbon components of the HTGR fuel must be burned. The quantity of gas is larger than that evolved from LWR or LMFBR processing and the composition is different since it is mostly CO_2. Although alternative processing schemes which propose the separation of the graphite by physical methods to make burning unnecessary have been suggested, the problems encountered (not the least of which was the storage of the contaminated graphite) appear more difficult than treatment of the burner off-gas. The burning operations are performed at temperatures between 700 and 1000°C with a slight excess of oxygen to avoid, insofar as possible, the formation of CO. Commercial oxygen would be used rather than air to avoid handling large quantities of N_2, but some inleakage of N_2 is unavoidable. It has been found[1] that several of the normally solid fission products are present in the off-gas at combustion conditions. The most important of the ones reported are Cs, Zr, Nb, Ru, and Ce, of which only the Ru exceeded (by a small amount) 10% volatilization. A sintered metal filter, located above the burner, was very effective in retaining all of these except Cs. About 2% of the Cs passed through a filter train, while the other metal fission products were retained with a decontamination factor greater than 10^3. The ^{3}H, Xe, and Kr were all quantitatively released in the burning operations. Data on I_2 are not available, but it is also expected to be released during burning. An estimated analysis of the gas stream after filtration is given in Table 1. For a 1-metric ton/day plant, the given numbers would be multiplied by 100 since 100 blocks would be processed per day.

Since the removal and handling of Kr seemed to be the most important problem, our attention has been directed to it. The available technology was thoroughly assessed to determine whether a process that would effectively accomplish this task existed.[2] However, we found that the processes which are practical for removing Kr from streams similar to contaminated air, without seriously altering the composition of the bulk stream, are ineffective for streams containing large amounts of CO_2. Indeed, the insidious similarity of the behavior of Kr and CO_2 usually establishes tolerable limits of CO_2 concentration in such processes. Sorption on molecular sieves or other solid sorbents, selective absorption by halocarbons, and selective membrane permeation techniques are among the processes eliminated by this factor.

The expedient of removing the CO_2 from the gas stream was then considered. This could be done by several methods. Reaction of the CO_2 with a lime bed produces prodigious amounts of solid radioactive waste for storage, and was thus ruled out. Caustic scrubbers are effective but also produce unacceptable amounts of waste. Among the regenerable scrubbing systems, the hot potassium carbonate system seems most desirable; specifically, it is as effective as, and more economical than, the amine sorbents. Finally, the possibility exists that the CO_2 could be removed by condensation. Because the triple point of CO_2 is -56.6°C at a vapor pressure of 5.1 atm, it is not feasible to completely remove the CO_2 as a liquid. In order to reduce the CO_2 content to a small fraction of the gas stream, desublimation temperatures of the order of -100°C are necessary even when the gas is compressed to a pressure of several atmospheres. None of the methods considered could ensure that the CO_2 removed from the gas stream would be sufficiently decontaminated from Kr or other fission products to allow its discharge. Further, the removal of CO_2 would not reduce the volume of the off-gas stream sufficiently to allow it to be stored, but would only prepare it for Kr removal by other methods.

Table 1. Estimated Burner Off-Gas Analysis[a]

Major Component	lb	scf	Mole Fraction
CO_2	1223	9976	0.897
O_2	75	846	0.075
N_2	24	312	0.028

Contaminant	ppm (total)	ppm (radioactive)	Curies
Krypton	16	1.2	572.0
Tritium	2.4×10^{-2}	2.4×10^{-2}	9.8
Iodine	3	9.2×10^{-7}	0.2
Xenon	61	—	—

[a] For head-end reprocessing of one FSVR fuel block; 6-year exposure, 150-day cooling.

This rather unpromising review of existing technology led us into the development of a rather unique method for removing Kr from the HTGR burner off-gas. This method, which involves the selective absorption of Kr in liquid CO_2, has been called the KALC (Krypton Absorption in Liquid Carbon Dioxide) process. The process operates at about 20-atm pressure and at temperatures from about -45°C to -20°C. The flowsheet, in simplified form, is shown in Fig. 1. The flow rates shown are those that might be used in a pilot facility and would be equivalent to processing three blocks of Ft. St. Vrain fuel per day. The flow ratios shown are approximate; however, more precise calculations, which continually change with incorporation of newly acquired data, show no qualitative differences.

Before being fed into the system, the filtered burner off-gas is compressed and chilled so that part of the CO_2 is condensed. In the absorber-fractionator system, virtually all of the Kr is selectively absorbed in the liquid phase, while all gas components with solubilities less than Kr (e.g., O_2, N_2 and CO) are returned to the gas phase and discharged from the top of the absorber along with much of the CO_2. Gases more soluble than Kr (e.g., Xe) follow the liquid CO_2 to the stripper, where the Kr is removed and concentrated. The CO_2 from the bottom of the stripper would contain components of low volatility. Xenon either could be allowed to accumulate in the CO_2 to the point where it is eventually discharged from the top of the absorber, or it could be removed by a separate distillation operation on the recycle CO_2 stream. This technique should yield a xenon product of very high purity.

The scrubber may be expected to remove from the incoming gas most of the particulates that reach the process. Under KALC conditions, water and all conceivable forms of iodine are essentially nonvolatile components, which, at the expected inlet concentrations, are soluble in the liquid phase. Solids and nonvolatile components would tend to accumulate in the recycled liquid CO_2. They could be removed by an evaporator, which would return purified CO_2 to the process and concentrate the solids for discharge. When it is realized that the volatilities of water and the iodine compounds are limited by the vapor pressure of the pure solid phases, one can imagine such an evaporator effectively operating with a thick slurry of crystals in the reboiler.

Development of the KALC process requires: (1) obtaining the necessary equilibrium and thermodynamic data for describing the system; (2) selecting, characterizing, and, in some cases, developing components required for a radiochemical application of the process; (3) selecting an effective operating mode with its associated control system; and (4) demonstrating the performance of an integrated system. At this time, items (2) and (3) have received only sufficient attention to assure us that appropriate solutions will be forthcoming. Work on items (1) and (4) has already yielded significant results.

Solubility of Krypton in Liquid CO_2

An experimental determination of the solubility of krypton in liquid CO_2 had been made at KFA Jülich previously,[3] but the results differed considerably from the solubility calculated by assuming ideal behavior. Therefore, we made our own measurements using in situ counting of tracer [85]Kr distributed between equilibrated gaseous and liquid phases in a sealed container. The in situ technique eliminated the inaccuracies usually associated with sampling highly volatile systems.
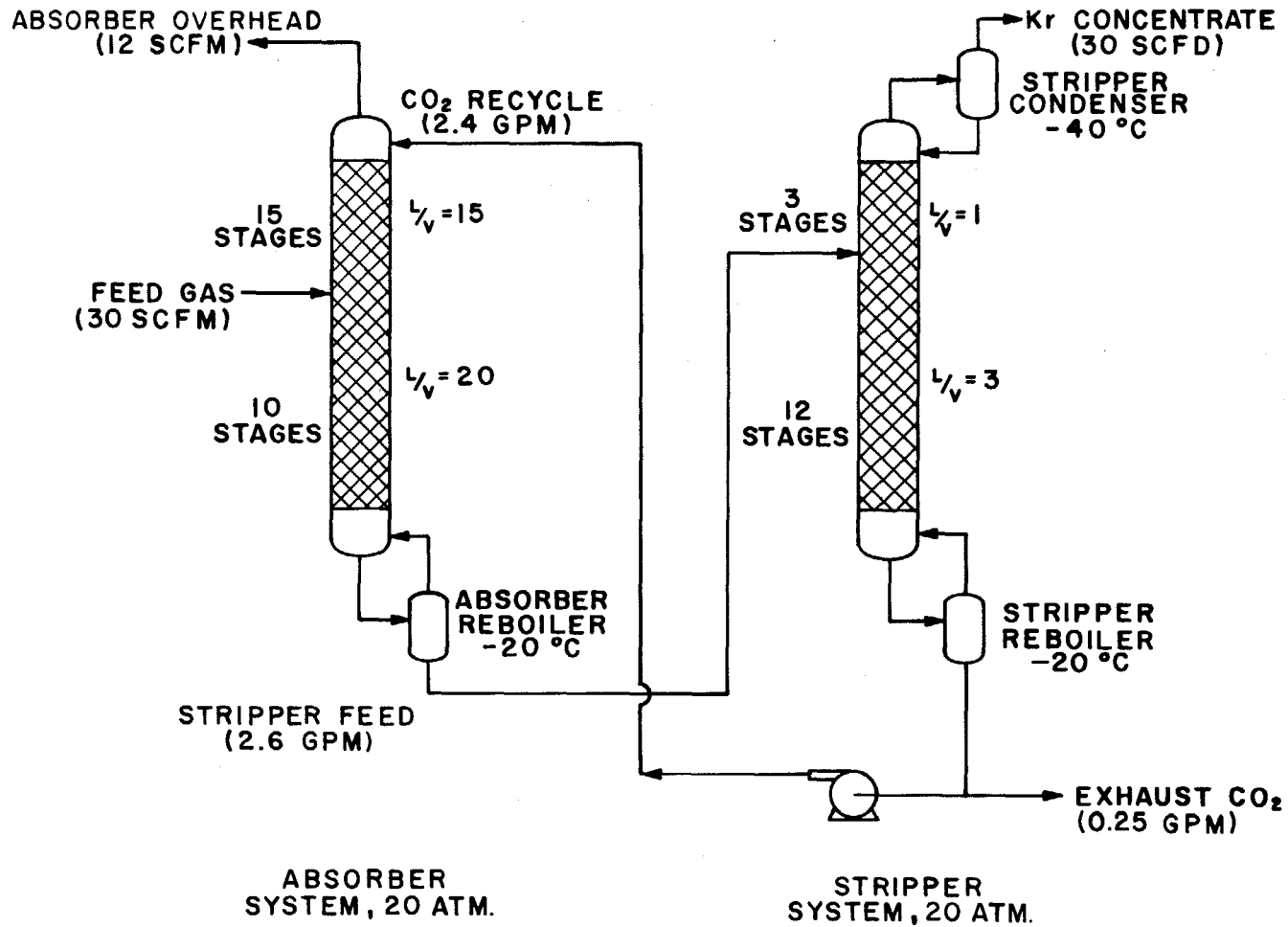
Fig. 1. Typical Flowsheet for the KALC Process.

The equipment used is shown schematically in Fig. 2. Essential components were a cold bath, an equilibrating device, and counting equipment. The temperature of the cold bath was controlled to within ±0.03°C by circulating a slight excess of coolant from a dry ice--trichlorethylene reservoir and supplying heat as called for by a thermostat. The Kr-CO_2 mixture was contained in a 1-in.-diam by 11-in.-long, stainless steel cylinder, which was rocked for at least 1 hr at temperature. We have determined that distribution equilibrium is attained by this procedure. The equilibrated system was then set upright, and the ^{85}Kr radioactivity was counted in each phase, yielding raw data on a volume basis. Data reduction involved correcting for internal attenuation and backscatter from the CO_2, and recalculating the Kr activity on a mole (rather than volume) basis. The correction, which was sometimes as much as 25% (depending on the CO_2 density and the gamma energy range counted), was made by means of a calibration curve. This curve was prepared empirically by incrementally adding CO_2 to a fixed quantity of Kr. The recalculation merely required the use of the CO_2 density, which is well known.
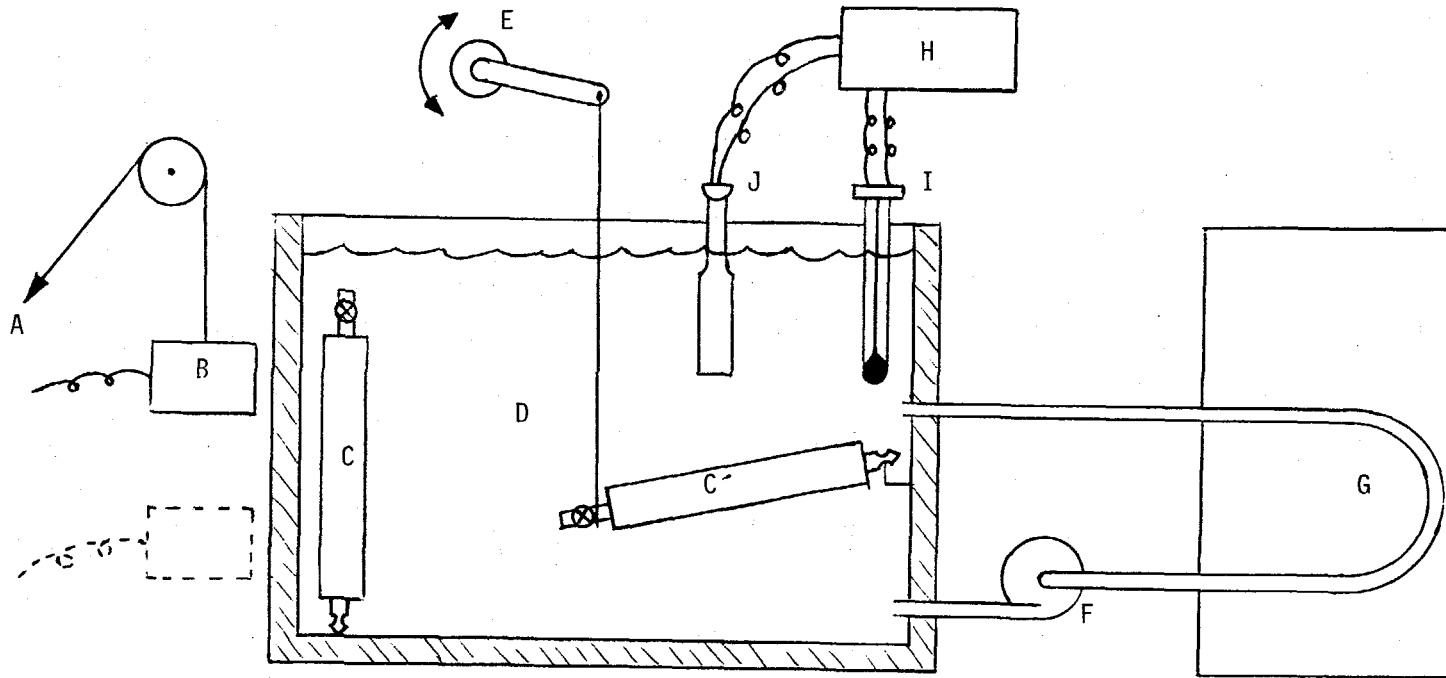
The data were finally expressed as a separation factor, Y_{Kr}/X_{Kr}, where Y and X are the mole fractions of Kr in the gaseous and liquid phases, respectively. The total Kr present (^{85}Kr plus nonradioactive Kr) was usually less than 1000 ppm; however, since the separation factor is a ratio, it was not necessary to know the exact amount. The reduced data are shown in Fig. 3. Fifty-nine data points, covering the entire liquid range, were obtained. The curve drawn through our data is linear over most of its length, showing a slight positive curvature near the triple point and dropping off strongly toward a value of unity as the critical temperature is approached. Our curve has about twice the slope of the calculated ideal curve and crosses it near 0°C. A more sophisticated calculated curve, which allows for nonideality in both phases,[4] falls below the ideal curve. The Jülich data tend to follow the latter curve but show a minimum at about 20°C. The fact that no minimum was predicted favors our results. Further, in order to validate the method used here, the distribution of ^{85}Kr in a Kr-H_2O system was determined and found to agree with reported values obtained by other methods.[5] Our known errors (from uncertainties in counting, temperature, CO_2 density, and empirical calibration) are somewhat less than the total scatter shown in Fig. 3.

Preliminary data indicate that the distribution of Kr is not significantly altered either at much higher Kr contents or by the presence of added oxygen.

Solubility of O_2, N_2, and CO in CO_2

The literature has provided a reasonable amount of data on the solubility of O_2 in liquid CO_2,[6-8] somewhat less on N_2 in CO_2[6,8,9] and a very small amount on CO in CO_2.[10] Most of the reported data were obtained at high concentrations, and hence at higher pressures than are of interest to this work. When the light gases comprise less than 50% of the gas phase, at total pressures less than 50 atm, the liquid phase contains less than 10% dissolved light gases. As the concentration of light gases decreases from this level, data become sparse and the accuracy diminishes; however, theoretical considerations have helped us to extrapolate the data into the low-concentration regions.

Equilibrium data from the literature have been fitted to a model which, over the range of conditions of interest, describes the KALC system quite satisfactorily. Of necessity, the model is based on binary system data. The only ternary data

A - Counterweight
B - Lead-shielded scintillation counter
C - Cylinder in counting position
C' - Cylinder in equilibrating position
D - Controlled temperature bath
E - Motor-driven oscillator

F - Circulating pump
G - Dry ice/solvent cold reservoir
H - Temperature controller
I - Sensing element
J - 250 watt heater

Fig. 2. Apparatus for in situ Measurement of Equilibrium Distribution of ^{85}Kr Between CO_2 Liquid and Gas Phases.
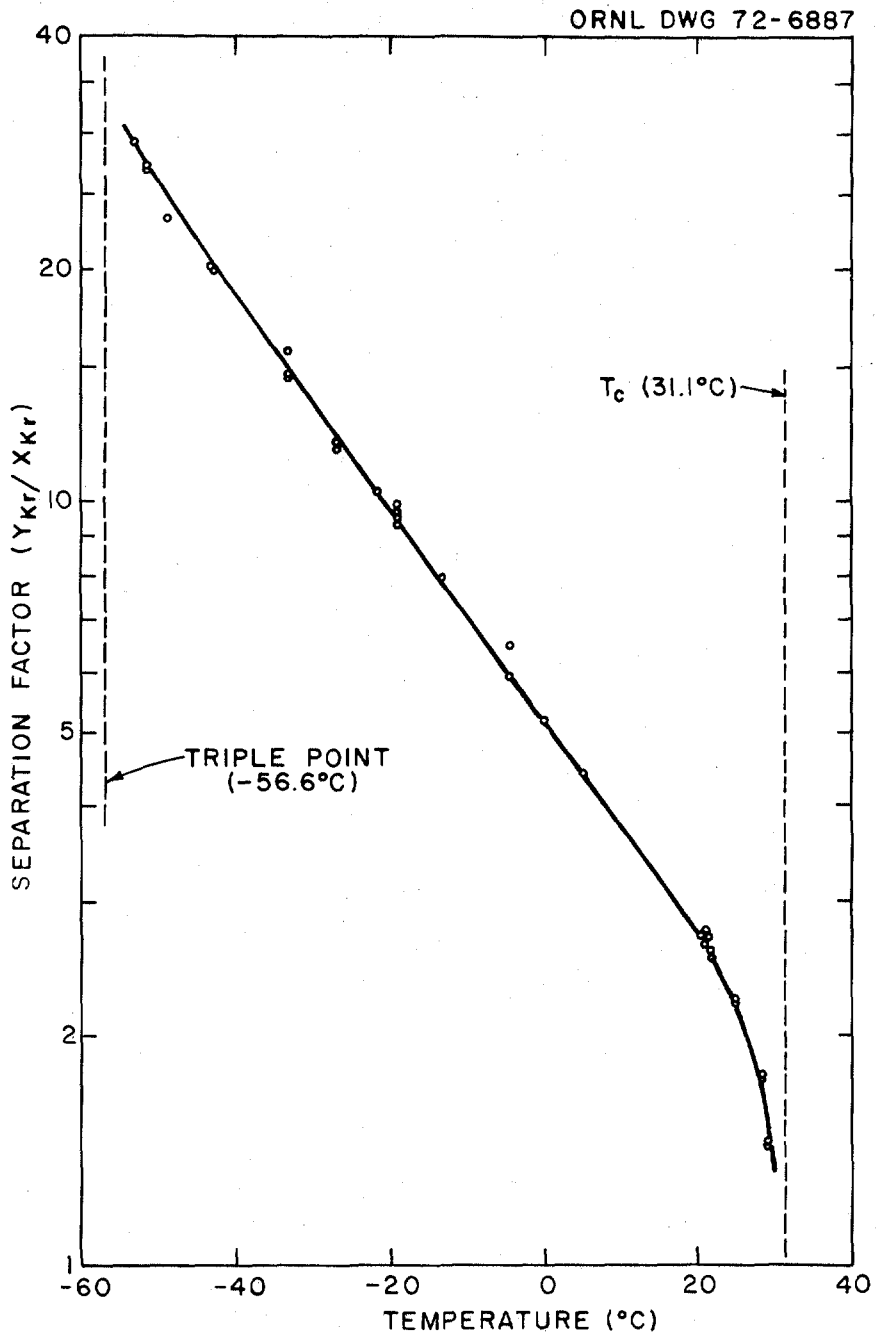
Fig. 3. Distribution of Krypton Between Gaseous and Liquid CO_2.

obtained under conditions close to those used for the KALC system were for the O_2-N_2-CO_2 system at pressures higher than 50 atm. Even though they were out of the proper range, these data and equilibrium numbers calculated from the model were in reasonable agreement. The model is most simply expressed in the following form: given a liquid phase composition and a temperature, calculate the total pressure and the vapor phase composition.

The total pressure was found to fit the empirical relation

$$P_t = P_{CO_2}^* + \Sigma a_i x_i + \Sigma b_i x_i P_{CO_2}^* + \Sigma x_j \Sigma c_i x_i, \tag{1}$$

where

P_t = total pressure (atm),

$P_{CO_2}^*$ = saturated vapor pressure of CO_2 at system temperature (atm),

x = mole fraction in liquid phase,

i,j = index subscripts applied to all components <u>except</u> CO_2,

a,b,c = empirically determined constants.

The compressibility of CO_2 vapor is such that a correction for nonideality is required. All other components have critical points sufficiently removed from KALC conditions that gas phase ideality can be assumed. A reasonable form for the gas phase composition then becomes:

$$y_{CO_2} = (p_{CO_2}/Z)/[\Sigma p_j + (p_{CO_2}/Z)] \tag{2}$$

$$y_i = p_i/[\Sigma p_j + (p_{CO_2}/Z)], \tag{3}$$

where

Z = the compressibility factor for saturated CO_2 at the temperature of the system,

p = partial pressure,

y = mole fraction in the vapor phase.

The partial pressures are defined so that

$$P_T = p_{CO_2} + \Sigma p_i. \tag{4}$$

Because the concentration of the dissolved light gases is small, Raoult's law was applied to the CO_2. It was necessary, however, to make a Poynting-type correction of the CO_2 vapor pressure. As an expedient in getting a better fit, the molar volume of the liquid phase was not used; instead, a fictitious molar volume about a factor of 3 times the real molar volume was employed.

The partial pressure of CO_2 is, then,

$$p_{CO_2} = P_{CO_2} (1 - \Sigma x_j), \tag{5}$$

where

$$P_{CO_2} = P_{CO_2}^* \exp[k(P_t - P_{CO_2}^*)/T], \tag{6}$$

94

and

$$P_{CO_2} = \text{effective vapor pressure of } CO_2 \text{ (atm)},$$

$T = \text{absolute temperature (°K)},$
$k = \text{a determined constant} = 1.7 \text{ °K/atm}.$

The partial pressure of the ith component is given by:

$$P_i = \frac{x_i}{\Sigma x_j} [P_{CO_2}^* - P_{CO_2} (1 - \Sigma x_j)] + a_i x_i + b_i x_i P_{CO_2}^* + c_i x_i \Sigma x_j. \tag{7}$$

For a binary system, Equation 7 reduces to:

$$P_i = P_t - (1 - x_i) P_{CO_2}. \tag{8}$$

These equations comprise a set from which equilibrium can be calculated. Table 2 gives the numerical values for the constants, along with the expressions used in this study to compute the compressibility factor, Z, and the saturated vapor pressure of CO_2, $P_{CO_2}^*$.

Henry's law constants consistent with the model, and defined as the limit of the ratio of the partial pressure to the mole fraction in the liquid phase, are shown in Fig. 4. It is noted that CO is predicted to be the most difficult component to separate from Kr, but only slightly more difficult than oxygen. The Kr-CO separation factor increases from 1.43 at 0°C to 1.8 at -20°C. These values are sufficiently high that neither the required height of towers nor the control of flow rates for KALC will cause undue concern.

Engineering Feasibility of the KALC Process

Despite the early stage of the development of KALC, the feasibility of the process has been demonstrated in a recent campaign conducted by ORNL at the ORGDP Rare Gas Removal Pilot Plant. The primary objective of this campaign was to establish our confidence in operating a liquid-CO_2--light-gas system. However, [85]Kr was used in tracer amounts during much of the operation.

The basic pilot plant, which has been used quite extensively over the past few years in the development of the fluorocarbon absorption processes,[11] is composed of three separate columns for carrying out the absorption, fractionation, and stripping operations. Each of the packed columns has a 9-ft section of packing; the absorber and the fractionator are each 3 in. in diameter, and the stripper is 10 in. in diameter.

A nominal gas flow of 10 to 15 scfm to the absorber, with a countercurrent flow of about 1.5 gpm of liquid CO_2, was used during the feasibility studies. Under these conditions and with an operating pressure of about 20 atm, the column temperatures were in the predicted range of -20 to -40°C. The system operated very smoothly throughout the campaign period (three weeks).

In-line analyses were not possible for checking concentrations, etc., but estimates (which were later verified by mass spectrographic analyses) leave little

Table 2. Coefficients Used to Correlate Equilibrium Data for the KALC System

Component i	a	b	c
O_2	532.33	-2.7153	-494.72
N_2	720.22	-5.9729	-553.88
CO	484.39	-1.8473	-395.10
Kr	188.0	2.80	—

Total Pressure $= P_t = P_{CO_2}^* + a_i x_i + b_i x_i P_{CO_2}^* + c_i x_i \Sigma x_j$

Henry's Constant $= H_i = a_i + P_{CO_2}^* (1 + b_i)$

Saturation Vapor Pressure of CO_2:

$$\ln (P_{CO_2}^*) = -8.175626 + 26.27742 \left(\frac{T}{600}\right) - 23.76839 \ln \left(\frac{T}{600}\right) - 8.62709785 \left(\frac{600}{T}\right)$$

Compressibility of $CO_2 = Z = 3.21203 - 0.029634967T + 1.3757 \times 10^{-4} T^2 - 2.2960 \times 10^{-7} T^3$
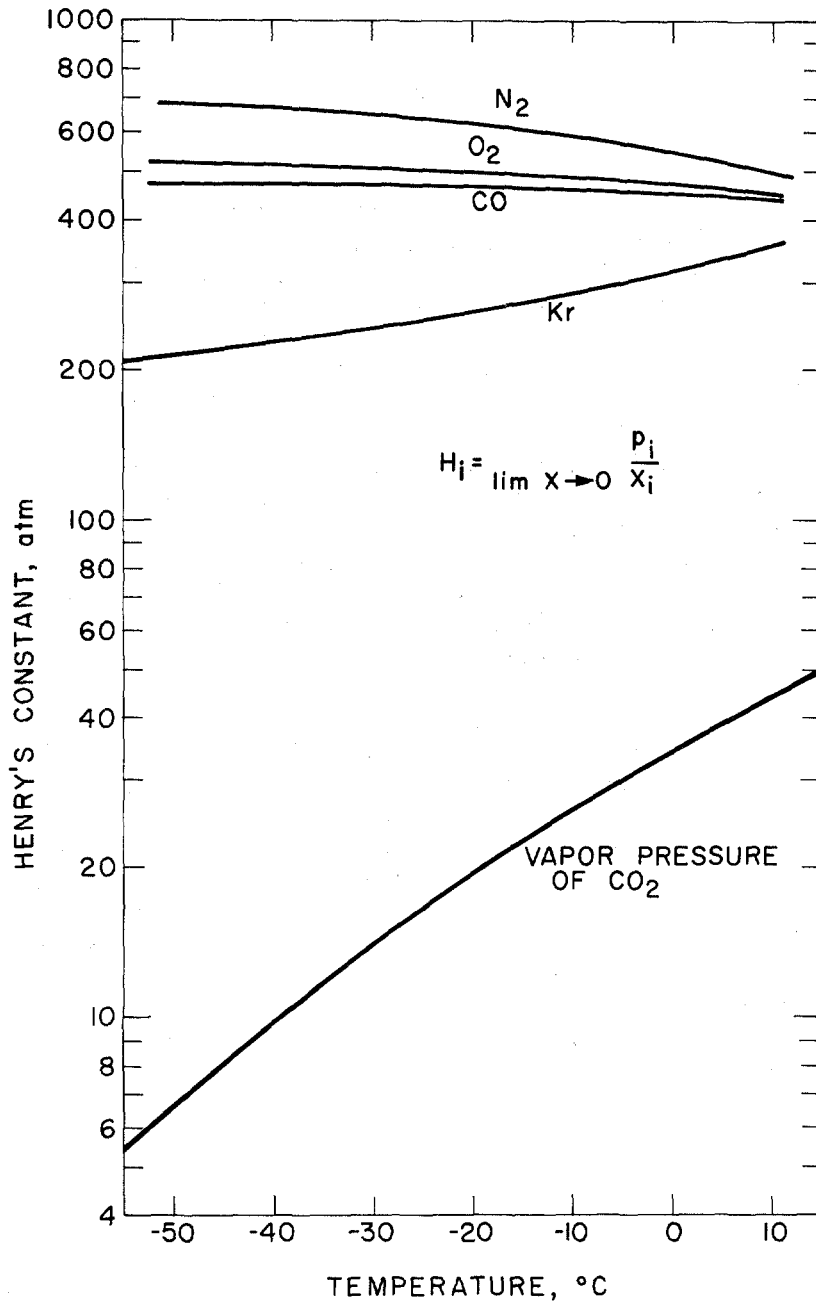
T = Absolute temperature (°K)

ORNL DWG 72-8787

Fig. 4. Henry's Constants for Major Components in the KALC Process.

doubt that such a system, with controls and instrumentation suited specifically to the liquid CO_2 process, can effectively remove Kr from the burner-type off-gases. Spot checks on the behavior of Kr in the system at arbitrary run conditions indicated both absorber and process DFs on the order of 100, with process concentration factors in excess of 1000.

Discussion

An economic evaluation of the KALC process has not yet been undertaken; thus specific costs are not yet available. The compressor and refrigeration requirements probably account for a major portion of the total expense for the KALC system, but even these costs will not be severe. The capital and operating costs associated with the KALC system should be only a small fraction of the costs for the rest of the reprocessing plant. Corrosion in the basic KALC process should present no problems. However, more study is required on corrosion in any special operation, such as one that would concentrate iodine and tritium for removal.

Many questions of an engineering nature are still unanswered; primarily, these questions are concerned with equipment design and performance, but they also include the selection of the operating mode most conducive to reliable control and system performance under transient loads. Preliminary analysis of the control problem indicated several plausible alternatives. A calculational model of the KALC process which can predict system performance will be valuable both in studying control and in interpreting the results of engineering experiments. Such a model is now partially complete.

Doubts about the feasibility of the KALC process have been dispelled by an actual demonstration in engineering equipment and by the accumulation and consideration of basic equilibrium and physical property data. We have yet to discover any supportable objection to the application of this process to HTGR off-gas decontamination. Our determination of the distribution of Kr in the KALC system and/or the data on the other light gases reported in the literature would have to be in error by at least a factor of 2 (which we consider incredible) to render the process unworkable. In summary, then, the advantages of using one of the components of the stream as the solvent to effect its decontamination, the moderate operating conditions employed, and the general effectiveness of the process make KALC very attractive.

Literature Cited

1. R. S. Lowrie, V. C. A. Vaughen, and C. L. Fitzgerald, "Determination of the Isotopes Present in the Off-Gas Streams Generated by the Head-End Steps in Reprocessing HTGR Type Fuels," paper presented at the 12th AEC Air Cleaning Conference, Aug. 28-31, 1972, Oak Ridge, Tenn.; to be published in the Proceedings.

2. R. W. Glass et al., HTGR Head-End Processing: A Preliminary Evaluation of Processes for Decontaminating Burner Off-Gas, ORNL-TM-3527 (July 1972).

3. KFA Jülich, Reprocessing of Thorium-Containing Nuclear Fuels, Progress Report for Second Half 1970, (February 1971), pp. 67-71.

4. W. Davis, Jr., Calculated Liquid-Vapor Equilibria in the Systems CO_2-Xe and CO_2-Kr at -55 to +5°C, ORNL-TM-3622 (December 1971).

5. GCR-TU Programs Ann. Progr. Rept. Sept. 30, 1971, ORNL-4760 (in press).

6. G. H. Zenner and L. I. Dana, "Liquid-Vapor Equilibrium Compositions of Carbon Dioxide-Oxygen-Nitrogen Mixtures," Chem. Eng. Progr., Symp. Ser. 59(44), 36-41 (1963).

7. A. Fredenslund and G. A. Sather, "Gas-Liquid Equilibrium of the Oxygen-Carbon Dioxide System," J. Chem. Eng. Data 15(1), 17-22 (1970).

8. G. Kaminishi and T. Toriumi, "Vapor-Liquid Equilibria Between Liquid Carbon Dioxide and Hydrogen, Nitrogen and Oxygen," Kogyo Kagaku Zashi 69(2), 175-78 (1966); also ORNL-tr-2615.

9. Y. Arai, G. Kaminishi, and S. Shozaburo, "The Experimental Determination of the P-V-T-X Relations for the Carbon Dioxide-Nitrogen and the Carbon Dioxide-Methane Systems," J. Chem. Eng. Japan 4(2), 113-22 (1971).

10. G. Kaminishi et al., "Vapor-Liquid Equilibria for Binary and Ternary Systems Containing Carbon Dioxide," J. Chem. Eng. Japan 1(2), 109-16 (1968).

11. M. J. Stephenson, J. R. Merriman, and D. I. Dunthorn, Experimental Investigation of the Removal of Krypton and Xenon from Contaminated Gas Streams by Selective Absorption in Fluorocarbon Solvents: Phase I Completion Report, ORGDP-K-1780 (Aug. 17, 1970).

DISCUSSION

LASER: In our lab, we have a poster which displays:
"Atomic Power means clean air." That's right. But we all know that
we must add: Reprocessing means emission of krypton, tritium, and
possibly 129 iodine.

A special problem of reprocessing is the decontamination of the
burner off-gas of THTR fuel. This is nearly the same as HTGR fuel,
which you have heard of. Therefore, since 1970, we have made theo-
retical studies and laboratory experiments of suitable processes to
retain volatile and non-volatile activity. During the last year we
have made several hot cell experiments and have installed a com-
plete decontamination process for hot cell experiments called AKUT.

Let me give you a short description of the results and of the
process. The composition of the burner off-gas differs considerably
depending on experimental conditions. The carbon monoxide content
fluctuates between approximately 5 and 25%. The activity, especi-
ally of 85 krypton, fluctuates by a factor of 10 or more during a
short time because of irregular burning of the coated particles.
Therefore, we have averaged measurements over an extended period to
arrive at mean values. In the case of carbide fuel elements the
burner off-gas activity is approximately 20 mCi/m^3 tritium,
420 mCi/m^3 krypton, and nearly 125 mCi/m^3 cesium. In the case of
oxide fuel elements, the emitted activity is lower; approximately by
a factor of 10.

Most of the off-gas activity is associated with aerosols,
especially cesium and iodine when short cooled fuel elements are
burnt. More than 99.8% of the cesium activity is separable by an
electrostatic precipitator. The iodine activity decontamination
factor has fluctuated between 2 and 2,000 because of different ratios
of particulate to molecular species. With absolute filters downstream
of the electrostatic separator, cesium activity can be reduced below
the maximum permitted concentration. The iodine activity, however,
remains high by a factor up to 1,000.

We have developed a process to separate krypton from the off-
gases by scrubbing with liquid carbon dioxide. We achieved decon-
tamination factors of 600 and more. In practice, because we have
a gas with fluctuating composition, control may be difficult. A
further problem is enrichment of krypton for storage and disposal.
We now prefer to liquify all of the off-gas by pressurizing at room
temperature and then, to enrich the krypton by rectification.

The hot cell experiments consist of the following steps:

(1) Precipitation of aerosols by an electrostatic separator.

(2) Decontamination of off-gases by an absolute filter. (We prefer
    a relatively clean off-gas before going into krypton separation.)

(3)   Oxidation of carbon monoxide with oxygen to give an off-gas with approximately 95% carbon dioxide and 5% oxygen.

(4)   Liquifying the off-gas by compression to approximately 70 atmospheres.

(5)   Enriching the krypton by rectification to approximately 10 to 20% krypton.

(6)   Further rectification to enrich tritiated water and, possibly, iodine at the bottom of the rectification column.

(7)   Evaporation of the tritium and iodine enriched solution and passing the gas over a tritium and iodine absorber.

A very coarse estimation of cost is 1.5×10^{-5} DM per KWH, but this value can be higher by a factor of 2.